1 # THERMAL-MECHANICAL BEHAVIOR OF COMPACTED GMZ BENTONITE

2

3 Yu-Jun Cui[i], Anh-Minh Tang[ii], Li-Xin Qian[iii], Wei-Min Ye[iv], Bao Chen[v]

4

5

6 ## *Abstract*

7 The THM behavior of compacted GMZ bentonite has been investigated using a
8 suction-temperature controlled isotropic cell. The results obtained were compared with the
9 existing results on other reference bentonites (MX80, FEBEX, FoCa, and Kunigel-V1). It has
10 been observed that the coefficient of thermal expansion of the compacted GMZ bentonite is 2
11 x 10^{-4}°C^{-1}, similar to the values of compacted MX80 and FEBEX bentonites. The heating tests
12 of the GMZ bentonite also show that the suction is an important parameter that governs the
13 thermal volumetric behavior of unsaturated soils. Unlike temperature, suction has a
14 significant effect on the compressibility parameters. Examination of the mineralogy of various
15 bentonites showed that a good correlation can be generally established between the
16 montmorillonite content and the cations exchange capacity (CEC) or the specific surface area
17 (S). Nevertheless, both the basic geotechnical properties and the swelling potential seem to
18 depend not only on the montmorillonite content but also on other factors such as the nature of
19 base exchangeable cations. The quartz content of the GMZ bentonite is relatively high
20 (11.7%). This could explain its relatively large values of thermal conductivity.

21

22 **Key words**: high-level radioactive waste disposals, compacted GMZ bentonite, suction,
23 temperature, thermo-mechanical behavior, comparison (IGC: D05/D08)

24

25

26 [i] Corresponding author, Professor, Tongji University, China, and Ecole des Ponts ParisTech,
27 U.R. Navier/CERMES, France
28 [ii] Researcher, Ecole des Ponts ParisTech, U.R. Navier/CERMES, France
29 [iii] PhD, Tongji University, China
30 [iv] Professor, Tongji University, China
31 [v] Associate professor, Tongji University, China

32

33

34 ## *Introduction*

35

36

37 Considering the key role played by the engineered barrier systems (EBS) in deep radioactive
38 waste disposals, notably related to i) isolation functions, ii) containment functions, and iii)
39 retrievability, compacted bentonites are often considered the best candidates for engineered
40 barrier materials. As an assessment of the EBS performance under complex
41 thermo-hydro-mechanical (THM) loadings is crucial in demonstrating the long-term safety of

1 disposal systems, large investigations are generally needed for a selected bentonite. The
2 experiments in these investigations must cover various scales, from small-scale elementary
3 laboratory tests through to mid-scale to large-scale tests in underground research facilities.
4 Various reference bentonites have been studied in various countries for this purpose:
5 Kunigel-V1 is used as the reference material for all the clay-based components in the
6 repository concepts in Japan (Sugita et al., 2007); MX80 was used in the Swedish prototype
7 repository project (Johannesson et al., 2007); the FoCa clay from the Paris Basin and the
8 Serrata clay from Spain (which is equally known as the FEBEX bentonite (Lloret and Villar,
9 2007) were considered in the RESEAL project performed in Belgium (Van Geet et al., 2007).
10   The preliminary long-term plan for the implementation of China's high-level radioactive
11 waste repository (Wang et al., 2006) suggests that a high-level radioactive waste repository
12 will be built in the middle of the 21st Century. In the Chinese concept of geological disposal,
13 bentonite has been selected as the buffer/backfill material. The Gaomiaozi (GMZ)
14 Na-bentonite taken from a large-scale deposit located in the North Chinese Inner Mongolia
15 Autonomous Region (300 km northwest of Beijing) has been chosen for this purpose. After
16 Wen (2006), preliminary research conducted on the swelling, mechanical, hydraulic, and
17 thermal properties have shown that the GMZ bentonite is a good buffer/backfill material.
18 Indeed, as reported by Wen (2006), it has relatively high thermal conductivity (K =
19 1.51 W/mK at a dry density of 1.6 Mg/m^3 and a water content of 26.7%), quite low water
20 permeability (at saturated state, k = 1.94 x 10^{-13} m/s at a dry density of 1.6 Mg/m^3 and a
21 temperature of 25 °C), a relatively high unconfined compression strength (1.74 MPa at a dry
22 density of 1.6 Mg/m^3 and a water content of 23.6%), and quite a high swelling pressure
23 (3.17 MPa at a dry density of 1.6 Mg/m^3). Chen et al. (2006) completed the experimental
24 investigation by determining the water retention curves of the GMZ bentonite and showed its
25 high retention capacity which is necessary for ensuring the containment function of the EBS.
26   Though sufficient preliminary experimental data have been obtained, allowing the
27 candidature of the GMZ bentonite to be retained, there is still a great need of experimental
28 data needed in terms of THM coupling behavior in order to confirm this candidature. In this
29 regard, there have been some results allowing a relevant analysis. In one study, Ye et al. (2009)
30 determined the unsaturated hydraulic conductivity of the GMZ bentonite under constant
31 volume conditions and they observed a strong coupling between water flux and mechanical
32 confining: the hydraulic conductivity determined was found first to decrease and then increase
33 with decreasing suction. The decrease can be attributed to the large pore clogging due to soft
34 gel creation by the exfoliation process. This coupling phenomenon was also observed on a
35 mixture of the Kunigel-V1/Hostun sand (Cui et al. 2008). In the present work, a
36 complementary study was performed to further investigate the coupled thermo-mechanical
37 behavior of the GMZ bentonite. The suction-temperature controlled isotropic cell developed
38 by Tang et al. (2007) was used for this purpose. The results obtained cover the swelling upon
39 wetting, the volumetric changes upon heating, and the compressibility at controlled suction
40 and temperature. Furthermore, the properties found for GMZ bentonite in this investigation
41 were compared with those of other reference bentonites available in the literature.
42

1 ## *Materials and methods*

2 *Materials*

3 Table 1 presents the mineralogical properties of the GMZ bentonite, as well as other reference

4 bentonites: the Kunigel-V1, FoCa, MX80 and FEBEX. These bentonites contain mainly

5 montmorillonite, which is an essential mineral to ensure sealing properties. Beside the

6 montmorillonite, there is quartz, which is also an important mineral for its particular influence

7 on thermal conductivity (Tang et al., 2008*b*). Note that a high thermal conductivity of the

8 engineered barrier allows the heat to dissipate quickly from the canisters, consequently

9 reducing the maximum temperature in the EBS. This is one of the reasons why sand/bentonite

10 mixtures are equally studied as buffer material in the repository concepts of Canada (Martino

11 et al., 2007) and Japan (Sugita et al., 2007).

12   The physical properties of GMZ bentonite are presented in Table 2. Compared to other

13 bentonites, GMZ bentonite has high montmorillonite content, which gives it a high Cations

14 Exchange Capacity (CEC = 77.30 meq/100g), a large plasticity index (I_p = 275), and a large

15 specific surface area (S = 570 m^2/g). Note also that the main base cations are Na and Ca.

16

17 *Methods*

18 As mentioned previously, the present work aims at investigating the thermo-mechanical

19 behavior of the GMZ bentonite. For the samples preparation, soil powder with an initial water

20 content of 12.2% was firstly compacted in an isotropic cell under a static pressure of 30 MPa.

21 The dry density after compaction was about 1.70 Mg/m^3. The compacted sample was then cut

22 and machined to obtain smaller samples of size 80 mm diameter and 10 mm high. All the

23 samples were then put in a sealed box with a relative humidity controlled by a saturated

24 solution of K_2CO_3 for about one week (see technical details in Delage et al., 1998). That

25 permitted an initial suction of 110 MPa to be imposed on the samples. The soil volume

26 changes during this suction initialization have been found to be negligible. That is in

27 agreement with the water retention curve obtained by Chen et al. (2006), showing a suction of

28 about 110 MPa at a water content of about 12% for a sample compacted to a dry density of

29 1.70 Mg/m^3.

30   The isotropic cell developed by Tang et al. (2007), which enables the study of mechanical

31 properties of compacted expansive soils using simultaneous control of suction and

32 temperature, was used in the present work. The basic scheme of the cell is presented in Fig. 1.

33 The soil specimen (80 mm in diameter and 10 mm high) was sandwiched between two dry

34 porous stones, both of which were embedded in metallic plates. Small holes (2 mm diameter)

35 were drilled in the lower plate, allowing the moisture exchange between the soil specimen and

36 chamber below the lower plate. A glass cup containing an over-saturated saline solution was

37 placed in the chamber to control the soil suction. A neoprene membrane (1.2 mm thick)

38 covered the soil specimen and the two metallic plates, avoiding any exchange between the

39 confining water in the cell and the soil pore water. A thermocouple installed inside the cell

40 was used to monitor the cell temperature, which was considered equal to the temperature of

41 the soil specimen during the test. The cell was immersed in a temperature-controlled bath

42 within a temperature fluctuation of ± 0.1 °C. A volume/pressure controller was used to apply

43 the confining pressure in the cell. This volume/pressure controller was also used to monitor

1 the volume change of the soil specimen through the volume change of the confining water in
2 the cell. During the test, volume and pressure readings of the volume/pressure controller as
3 well as the cell temperature were recorded by a computer.
4 Following the tests carried out by Tang et al. (2008*a*) on compacted MX80 bentonite,
5 thermal loadings were applied over a short duration of less than 24 h, and the soil suction was
6 assumed to remain unchanged within this short time. The soil suction was then equal to the
7 total suction imposed by the saturated salt solution. Tang and Cui (2005) measured the
8 suctions generated by saturated salt solutions at different temperatures, and these results were
9 applied in this investigation to determine the imposed suction at a given temperature. The
10 saturated salt solution, which filled the glass cup of the cell, was chosen according to the
11 desired values of suction and temperature during the test. Three suctions were considered: 9
12 MPa (KNO_3 at 25 °C and K_2SO_4 at 60 °C); 39 MPa (NaCl at 25 °C and 60 °C); and 110MPa
13 (K_2CO_3 at 25 °C, $MgNO_3$ at 60 °C).
14 For tests at suctions lower than the initial suction of 110 MPa, the total suction was
15 initially imposed outside the cell by putting the samples in a sealed box containing saturated
16 KNO_3 solution (9 MPa suction) or NaCl solution (39 MPa suction). The soil sample volume
17 change due to this suction decrease was monitored using a precision caliper. The mass of the
18 soil sample was determined every 3 days until it reached a stable value. The sample was
19 installed inside the isotropic cell only after this suction equilibrium process. Prior to the test,
20 the dimensions of the sample were adjusted to fit the required size (80 mm in diameter and 10
21 mm high).
22 A total of six tests were performed (T1 to T6) and their stress paths are presented in Table
23 3 and Fig. 2, in a space of total suction (*s*), pressure (*p*) and temperature (*T*). During a
24 mechanical compression test the cell pressure was increased in steps from 0.1 to 0.2, 0.5, 1, 2,
25 5, 10, 20 and 50 MPa. The volume change of water in the volume/pressure controller was
26 recorded for each step. Calibration tests at various temperatures and pressures were performed
27 with a metallic specimen that had the same dimensions as the soil specimen. An example of
28 the determination of soil volume change for a loading step from 1 to 2 MPa (test T1) is shown
29 in Fig. 3. The deformation of the metallic specimen was assumed to be negligible within this
30 range of pressure (lower than 50 MPa) and the water volume change recorded during the
31 calibration corresponds mainly to the deformation of the cell and the tubing. The volume
32 change of the soil sample was then deduced from the difference between the calibration curve
33 and the curve from test, as depicted in Fig. 3. This volume change was used to calculate the
34 volumetric strain of the soil sample upon mechanical loading.
35 Fig. 4 shows the determination of the soil volume change during heating from 25 °C to
36 60 °C under a constant pressure of 0.1 MPa (test T4). Upon heating, the water in the cell
37 expanded and moved into the volume/pressure controller. According to Romero et al. (2005),
38 the thermal expansion coefficient of compacted expansive soil is approximately 10^{-4} °C^{-1},
39 much higher than the metal specimen (10^{-6} °C^{-1}) used for the calibration. Thus, it can be
40 reasonably assumed that the thermal expansion of the metal was negligible in comparison
41 with that of the soil. The soil volume change during heating can be then determined from the
42 difference between two curves obtained during the calibration and the test (Fig. 4*a*). In the
43 case of test T4 while heating from 25 to 60 °C, the soil volume increased by 310 mm^3 (Fig.
44 4*b*), which corresponds to a volumetric strain ε_v of -0.622%.

1

Experimental results

Soil volume change during the initial humidification

Fig. 5 shows a typical result of volumetric strain of the soil specimens due to wetting from the initial suction (110 MPa) to 39 and 9 MPa, as well as axial and radial strains. It can be seen that the radial strain is almost equal to the axial strain, showing isotropic behavior in the soil specimen. This observation is consistent with the procedure of compaction under isotropic pressure adopted for the specimen preparation. A similar observation was also made by Tang et al. (2008*a*). Furthermore, it can be noticed that the total volume of the soil specimen is increased by 32.9% when the suction is decreased to 9 MPa from 110 MPa.

Volume change under thermal loading

As shown in Fig. 2, the initial state was defined by zero pressure, 25 °C temperature and 110 MPa suction. For test T4, the soil specimen in its initial state was confined to a pressure p = 0.1 MPa, and heated to a temperature T = 60 °C under p = 0.1 MPa. For test T5, a decrease of suction from 110 to 39 MPa at T = 25 °C was first undertaken during the initial wetting before the application of the confining pressure p = 0.1 MPa; heating to T = 60 °C then followed. For test T6, the soil specimen was wetted to a suction of 9 MPa and then loaded to p = 0.1 MPa and heated to T = 60 °C.

Fig. 6 shows the results for the thermal volume change under p = 0.1 MPa. The results from tests T4 (110 MPa) and T5 (39 MPa) show that heating induces expansion and the coefficients of thermal expansion is $\alpha = 2\times10^{-4}$ °C^{-1}. On the contrary, the result from test T6 (9 MPa) shows a volume decrease upon heating.

Volume change under mechanical loading

As shown in Fig. 2, the mechanical loadings in tests T1-T5 were performed at constant suction and temperature. Two temperatures (25 and 60 °C) and three suctions (110, 39 and 9 MPa) were applied. The results (the void ratio e against the logarithm of pressure log$p$) for all these tests are presented in Fig. 7. The compressibility parameters, such as the yield pressure p_0, defined as the pressure at the intersection between the two quasi-linear segments, the elastic compressibility parameter, κ, which is related to the slope of small changes in the void ratio, and the plastic compressibility parameter, $\lambda(s)$, which is related to the slope of large changes in void ratio, can be determined from these curves. It is to be noted that the notations defined by Alonso et al. (1990) are adopted here for the compressibility parameters.

From Fig. 7*a* it can be observed that temperature increase from 25 °C to 60 °C raises the void ratio from 0.508 to 0.518 at a pressure of 0.1 MPa and constant suction of 110 MPa. Furthermore, there is no increase in the void ratio due to the temperature change after a pressure of 11 MPa. This indicates thermal expansion due to heating at low pressure which is consistent with the results shown in Fig. 6. The effect of heating on volume change is much smaller than the volume change under subsequent mechanical loading. This phenomenon can be observed again at constant suction of 39 MPa, as depicted in Fig. 7*b*. Heating from 25 °C to 60 °C slightly increased the void ratio e from 0.754 to 0.768. Again, the volume change due

1   to heating is small compared to that due to subsequent mechanical loading. When comparing

2   the compression curves of T2 (25 °C) and T5 (60 °C), it is observed that the difference is not

3   significant. Moreover, the shape of the compression curve is similar to that obtained for T1

4   and T4. At 9 MPa suction, only one loading test was performed (T3); a technical problem

5   occurred during test T6. The compression curve for test T3 is presented in Fig. 7*c*.

6   Though the temperature effects on $\lambda(s)$ and κ are found to be negligible, this is not the

7   case for the suction effect. Indeed, Fig. 8 shows that $\lambda(s)$ and κ increase significantly when the

8   suction is decreased. When the suction is decreased from 110 to 9 MPa, κ increases from

9   0.023 to 0.036 and $\lambda(s)$ increases from 0.120 to 0.165. Fig. 9 shows the yield pressures p_0

10   determined from Fig. 7 at various suctions and temperatures. It can be seen that p_0 decreases

11   from 21 MPa at the initial suction $s = 110$ MPa to 10 MPa at $s = 39$ MPa and 2 MPa at $s = 9$

12   MPa for the tests at 25 °C. As far as the temperature effect is concerned, at $s = 110$ MPa,

13   heating from T= 25 °C to 60 °C decreases p_0 from 21 to 16 MPa. At $s = 39$ MPa heating

14   decreases p_0 from 10 to 7.3 MPa.

15

Discussions

16

17   In this section the thermo-mechanical behavior of the GMZ bentonite identified will be

18   discussed by comparing it with that of other reference bentonites (listed in Table 1) which

19   have been studied worldwide.

20

21   *Mineralogical properties*

22   Table 1 shows that the montmorillonite content of the GMZ bentonite is lower than that of the

23   MX80 bentonite and the FEBEX bentonite but it is higher than that of the Kunigel-V1

24   bentonite. The FoCa bentonite contains 80% of interstratified smectite/kaolinite. The quartz

25   content of the Kunigel-V1 and the GMZ bentonites is relatively high: 29-38% and 11.7%

26   respectively (smaller than 6% for the others). Good correlations can be established between

27   the montmorillonite content and the CEC values (Fig. 10*a*). Indeed, the higher the

28   montmorillonite content, the larger the CEC; the FEBEX bentonite with the highest

29   montmorillonite content has the largest values of CEC. The FoCa clay with an 80%

30   interstratified smectite/kaolinite content is not considered in these correlations. As far as the

31   other properties are concerned (Table 2), it seems that the specific surface area (S), liquid

32   limit (w_L) and the plasticity index (*Ip*) are not directly related to the montmorillonite content

33   (Fig. 10*b,c,d*). For instance, the FEBEX bentonite with the highest montmorillonite content

34   has the smallest values of w_L and Ip while the MX80 bentonite (79% montmorillonite) has the

35   highest values of w_L and Ip. This shows that the montmorillonite content is not the only factor

36   which influences the basic geotechnical properties; other factors, such as the nature of the

37   base cations exchange (see Table 2), must play an important role also.

38

39   *Thermal conductivity*

40   Tang et al. (2008*b*) studied the thermal conductivity of the compacted MX80, FEBEX and

41   Kunigel bentonites. Tests on the compacted specimens having various dry densities (ranging

42   from 1.45 to 1.85 Mg/m^3) and water contents show that the thermal conductivity of bentonites

1 is strongly dependent on these two parameters: at the same water content, the higher the density
2 the higher the thermal conductivity, and at the same dry density, the higher the water content,
3 the higher the thermal conductivity. After testing various models for predicting the thermal
4 conductivity, Tang et al. (2008*b*) found that a unique relationship can be established between
5 the thermal conductivity K and the air-pore volume fraction V_a/V for all these soils, as follows:

6 $$K = \alpha(V_a/V) + K_{sat} \qquad (1)$$

7 where α is the slope of $K - V_a/V$ plot; K_{sat} is the thermal conductivity at saturated state which
8 corresponds to the intersection of $K - V_a/V$ plot with the K axis.
9   Fig. 11 shows the $K - V_a/V$ plot for the compacted GMZ bentonite that was drawn using
10 data reported by Wen (2006). It can be seen that there is also a good linear relationship for this
11 bentonite. From Fig. 11 the parameters of Eq. [1] deduced are as follows:

12 $\alpha = -2.81$ W/mK and $K_{sat} = 1.57$ W/mK

13   These values are slightly larger than those for other bentonites: FEBEX ($\alpha = -2.29$ W/mK

14 and $K_{sat} = 1.30$ W/mK), MX80 (α = -1.79 W/mK and K_{sat} = 1.1 W/mK), Kunigel V1

15 ($\alpha = -2.36$ W/mK and $K_{sat} = 1.39$ W/mK). Even though relatively larger values of the

16 thermal conductivity at saturated state (K_{sat}) for the GMZ and Kunigel-V1 bentonites can be
17 related to their higher quartz contents (see Table 1), it appears that the difference is too small to
18 allow establishing a relevant correlation. Further study is needed to clarify this phenomenon by
19 working on the different bentonites but using the same test protocol and measurement
20 technique.
21
22 *Swelling behavior*
23 Fig. 5 shows that for the GMZ bentonite compacted at 1.70 Mg/m^3 of dry density (initial
24 suction of 110 MPa), wetting to suction at 9 MPa induced a swelling volumetric strain of
25 32.9%. The volumetric swelling strain of GMZ is plotted together with that of other soils in
26 Fig. 12. A higher value of 50% was obtained by Tang et al. (2008*a*) when wetting from a
27 suction of 110 MPa to 9 MPa the MX80 bentonite compacted at 1.78 Mg/m^3 of dry density.
28 Delage et al. (1998) showed that wetting the compacted FoCa clay (1.85 Mg/m^3 of dry density,
29 initial suction of 110 MPa) to a suction of 9 MPa induced a volumetric strain of 17%. After
30 ENRESA (2000), wetting the FEBEX bentonite (initially compacted at 1.67 Mg/m^3 of dry
31 density) from a suction of 110 MPa to a suction of 9 MPa induced a volumetric strain of 19%.
32 Kanno and Wakamatsu (1993) studied the volume change behavior of the compacted Kunigel
33 V1 (initially compacted at 1.82 Mg/m^3 of dry density) and obtained a volumetric strain of
34 13% when wetting from 110 to 9 MPa suction. The comparison shows that the swelling
35 potential of the GMZ and the MX80 is higher than that of FoCa, Kunigel-V1 and FEBEX.
36 This is due to their montmorillonite contents (a higher montmorillonite content gives rise to a
37 higher swelling potential, see Marcial et al. 2002) and the nature of exchangeable basic
38 cations (Na-based bentonites show higher swelling potential than Ca-based bentonites, see
39 Marcial et al. 2002).
40

1   *Thermal-mechanical volume changes*

2   The coefficient of thermal expansion of the compacted GMZ bentonite deduced from Fig. 6 is

3   $2 \times 10^{-4} °C^{-1}$ (mean value determined from the thermal expansion curve of tests T4 and T5).

4   Similar values were obtained for the compacted MX80 bentonite (Tang et al., 2008*a*) and the

5   compacted FEBEX bentonite (Romero et al., 2005). As far as the nature of the volume

6   changes upon heating is concerned, Tang et al. (2008*a*) observed that heating the compacted

7   MX80 bentonite under 0.1 MPa pressure gave rise to thermal expansion at high suctions (39

8   and 110 MPa) and to thermal contraction at a lower suction (9 MPa). The same phenomenon

9   was observed in the present work on the GMZ bentonite. This behavior was explained using

10 an elasto-plastic constitutive model proposer by Tang & Cui (2009). The thermal expansion

11 corresponds to an elastic behavior when the heating path remains in the elastic zone while the

12 thermal contraction corresponds to a plastic behavior when the heating path under constant

13 stress and suction touch the yield surface.

14   The compression curves obtained at controlled suction and temperature (Fig. 7) show an

15 elasto-plastic behavior with a clear change in slope. That allowed the determination of the

16 compressibility parameters: κ, $\lambda(s)$ and p_0. Similar observations were made by Tang et al.

17 (2008*a*) on the MX80 bentonite and by Lloret et al. (2004) on the FEBEX bentonite. The

18 plastic behavior in compacted soil is usually associated with the collapse of macro-pores that

19 can be evidenced by MIP (Mercury Intrusion Porosimetry) test as in the works of Lloret et al.

20 (2003), Tang & Cui (2009), and Tang et al. (2011). However, Cui et al. (2002) performed

21 suction-controlled isotropic compression tests on the highly compacted FoCa clay (compacted

22 initially at 1.85 Mg/m^3 of dry density) and observed a reversible volume change behavior in a

23 range of pressures up to 60 MPa. The authors explained this by the absence of collapsible

24 macro-pores in this material. That mean the volume change behavior of compacted clays can

25 be strongly dependent on the dry density; the higher the dry density (or the lower the volume

26 of macro-pores) the higher the yield stress. Note that the initial dry densities of bentonite in

27 other studies are lower than in Cui et al. (2000): 1.70 Mg/m^3 for FEBEX bentonite in Lloret et

28 al. (2003); 1.78 Mg/m^3 for MX80 bentonite in Tang & Cui (2009). In the study of Tang et al.

29 (2011), even at a high dry density of 2.00 Mg/m^3, the volume of macro-pores measured by

30 MIP tests is still high. It shows that isotropically compacting GMZ bentonite at 30 MPa

31 pressure (to a dry density of 1.70 Mg/m^3) can not avoid macro-pores. Further study is

32 necessary to clarify this point.

33   The effects of suction and temperature on κ and $\lambda(s)$ of GMZ bentonite are similar to that

34 of MX80: κ and $\lambda(s)$ increase with the decrease of suction but are independent of the

35 temperature changes (between 25 and 60 °C). Lloret et al. (2004), however, observed that

36 both the increase of temperature and the decrease of suction induced an increase of $\lambda(s)$ in

37 FEBEX bentonite. Comparing the values of $\lambda(s)$, GMZ bentonite shows the highest values: $\lambda(s)$

38 = 0.12 – 0.16 at s = 9 – 110 MPa for GMZ bentonite; $\lambda(s)$ = 0.08 – 0.12 at s = 9 – 110 MPa for

39 MX80 bentonite; $\lambda(s)$ = 0.065 -0.080 at s = 8 - 14 MPa for FEBEX bentonite (from

40 suction-controlled oedometer tests by Lloret et al., 2003).

41   The effect of temperature on the yield stress p_0 of GMZ bentonite and MX80 bentonite

42 (see Tang et al. 2008*a*) is similar; only a slight decrease of p_0 was observed for high suction

43 values (s = 110 and 39 MPa). In contrast, for FEBEX bentonite, at s = 120 MPa, Lloret et al.

44 (2004) showed that p_0 decreased drastically from 20 MPa (at 20°C) to 3 MPa (at 50 °C).

1   In order to compare the effect of suction decrease on the yield stress, the results of three
2   bentonites (GMZ, MX80 and FEBEX) are plotted together in Fig. 13. At high suctions (s =
3   110 – 127 MPa), the yield stresses of the three soils are close to 20 MPa. Upon wetting, the
4   yield stress decreases in similar pattern for GMZ bentonite and FEBEX bentonite but at a
5   lower rate than MX80 bentonite: at s = 9 MPa, p_0 of GMZ and FEBEX bentonites decreases
6   to 2 MPa while that of MX80 is much lower (0.38 MPa).

Conclusions

9   The thermo-mechanical behavior of GMZ bentonite, which has been selected as a possible
10   material for the engineered barriers in the high-level radioactive waste disposals in China, was
11   experimentally investigated. The results obtained were compared with other bentonites which
12   have been widely investigated as reference materials in the projects carried out in other
13   countries (MX80, FEBEX, FoCa, and Kunigel-V1). The following conclusions can be drawn
14   from the present study:
15   i)   The montmorillonite content of GMZ bentonite is lower than that of MX80 bentonite
16   and FEBEX bentonite but it is higher than that of Kunigel-V1 bentonite. That explains
17   the large values of its cations exchange capacity (CEC) and specific surface area S. In
18   general, good correlations can be established between the montmorillonite content and
19   the CEC values or the specific surface area S (Table 2). Nevertheless, no direct
20   correlation can be made between the montmorillonite content and the basic geotechnical
21   properties; other factors, such as the nature of base exchangeable cations, also appear to
22   have a significant influence.
23   ii)   The same observation has been made in terms of swelling potential. In general, the
24   higher the montmorillonite content, the higher the swelling potential. However, a
25   Ca-based bentonite generally shows lower swelling potential than a Na-based bentonite.
26   For GMZ bentonite it was observed that wetting (suction decreased from 110 to 9 MPa)
27   induced a swelling volumetric strain of 30%. That is lower than MX80 (50%) and
28   higher than that of other bentonites (less than 20%).
29   iii) The quartz content of GMZ bentonite is relatively high (11.7%) just behind Kunigel V1
30   bentonite (29-38%). This could explain their relatively large values of thermal
31   conductivity. Note that compared to the values for other bentonites, the difference is too
32   small to allow for a relevant correlation to be drawn between their thermal conductivity
33   and the quartz content.
34   iv)   The coefficient of thermal expansion of the compacted GMZ bentonite is $2.10^{-4\circ}C^{-1}$, that
35   is similar to the values obtained for the compacted MX80 bentonite (Tang et al., 2008a)
36   and the compacted FEBEX bentonite (Romero et al., 2005). As the compacted MX 80
37   bentonite, the GMZ bentonite also showed a thermal expansion upon heating at high
38   suctions (39 and 110 MPa) and a thermal contraction at lower suction (9 MPa).
39   v)   The effect of suction and temperature on κ and $\lambda(s)$ of GMZ bentonite is similar to
40   MX80: κ and $\lambda(s)$ increase with decreasing suction but are independent of the
41   temperature changes. Compared to other bentonites, GMZ bentonite has the highest
42   values of $\lambda(s)$: 0.12 – 0.16 at s = 9 – 110 MPa.

vi) The effect of temperature on the yield stress p_0 of the GMZ bentonite has been found to be insignificant. A similar observation was made for MX80 bentonite by Tang et al. (2008*a*). In contrast, a significant suction effect was identified. As is also the case for MX80 bentonite and FEBEX bentonite, the yield stress p_0 of the GMZ bentonite decreased significantly, at a rate similar to that of FEBEX bentonite but lower than that of MX80 bentonite.

Acknowledgements

References

Alonso, E.E., Gens, A. and Josa, A. 1990. A constitutive model for partially saturated soils. Géotechnique, **40** (3): 405-430.

Chen, B., Qian, L.X., Ye, W.M., Cui, Y.J. and Wang, J. 2006. Soil-water characteristic curves of Gaomiaozi bentonite. Chinese Journal of Rock Mechanics and Engineering, **25**(4): 788 – 793.

Cui, Y. J., Sultan, N. and Delage, P. 2000. A thermo-mechanical model for saturated clays. Can. Geotech. J., **37**(3): 607-620.

Cui, Y.J., Yahia-Aissa, M. and Delage, P. 2002. A model for the volume change behaviour of heavily compacted swelling clays. Engineering Geology, **64** (2): 233 – 250.

Cui, Y.J., Tang, A.M., Loiseau, C. and Delage P. 2008. Determining the unsaturated hydraulic conductivity of a compacted bentonite-sand mixture under confined and free-swell conditions. Physics and Chemistry of the Earth, **33** (S1): S462 – S471.

Delage, P., Howat, M.D., and Cui, Y.J. 1998. The relationship between suction and swelling properties in a heavily compacted unsaturated clay. Engineering Geology, **50** (1): 31-48.

ENRESA, 2000. Full-scale engineered barriers experiment for a deep geological repository for high-level waste in crystalline host rock. Final Report. Technical Publication ENRESA 01/2000, Madrid, 354 pp.

Guillot, X., Al-Mukhtar, M., Bergaya, F. and Fleureau, J.M. 2002. Estimation de la porosité dans un matériau argileux. C.R. Geoscience, **334** : 105 – 109.

JNC 2000. H12 Project to establish technical basis for HLW disposal in Japan, Supporting report 3, Safety assessment of the geological disposal system. JNC Tech. Rep., JNC TN1410 2000-004.

Johannesson, L. E., Börgesson, L., Goudarzi, R., Sandén, T., Gunnarsson, D. and Svemar, C. 2007. Prototype repository: A full scale experiment at Äspö HRL. Physics and Chemistry of the Earth, **32**: 58-76.

Kanno,T. and Wakamatsu, H. 1993. Moisture adsorption and volume change of partially saturated bentonite buffer materials. Materials Research Society Symposia Proceedings,

294: 425-430.

Komine, H. 2004. Simplified evaluation on hydraulic conductivities of sand-bentonite mixture backfill. Applied Clay Science, **26** (1-4): 13 – 19.

Lloret, A. and Villar, M.V. 2007. Advances on the knowledge of the thermo-hydro-mechanical behaviour of heavily compacted "FEBEX" bentonite. Physics and Chemistry of the Earth, **32**: 701-715.

Lloret, A., Villar, M. V., Sanchez, M., Gens, A., Pintado, X. and Alonso, E. E. 2003. Mechanical behaviour of heavily compacted bentonite under high suction changes. Géotechnique, **53**(1): 27-40.

Lloret, A., Romero, E. and Villar, M.V. 2004. FEBEX II Project. Final report on thermo-hydro-mechanical laboratory tests. ENRESA technical publication 10/2004.

Marcial, D., Delage, P. and Cui, Y.J. 2002. On the high stress compression of bentonites. Canadian Geotechnical Journal, **39**: 812 -820.

Martino, J. B., Dixon, D. A., Kozak, E. T., Gascoyne, M., Vignal, B., Sugita, Y., Fujita, T. and Masumoto, K. 2007. The tunnel sealing experiment: An international study of full-scale seals. Physics and Chemistry of the Earth, **32**: 93-107.

Montes-H., G., Duplay, J. Martinez, L. and Mendoza, C. 2003. Swelling-shrinkage kinetics of MX80 bentonite. Applied Clay Science, **22**: 279 – 293.

Romero, E., Villar, M. V. and Lloret, A. 2005. Thermo-hydro-mechanical behaviour of heavily overconsolidated clays. Engineering Geology, **81**: 255-268.

Sugita, Y., Fujita, T., Takahashi, Y., Kawakami, S., Umeki, H., Yui, M., Uragami, M. and Kitayama, K. 2007. The Japanese approach to developing clay-based repository concepts – An example of design studies for the assessment of sealing strategies. Physics and Chemistry of the Earth, **32**: 32-41.

Tang, A. M. and Cui, Y. J. 2005. Controlling suction by the vapour equilibrium technique at different temperatures and its application in determining the water retention properties of MX80 clay. Canadian Geotechnical Journal, **42** (1): 287-296.

Tang, A.M., Cui, Y.J. 2009. Modelling the thermo-mechanical behaviour of compacted expansive clays. Géotechnique, **59** (3): 185-195.

Tang, A. M., Cui, Y. J. and Barnel, N. 2007. A new isotropic cell for studying the thermo-mechanical behavior of unsaturated expansive soil. Geotechnical Testing Journal, **30** (5): 341-348.

Tang, A. M., Cui, Y. J. and Barnel. N. 2008*a*. Thermo-mechanical behaviour of a compacted swelling clay. Géotechnique, **58** (1): 45-54.

Tang, A. M., Cui, Y. J. and Le, T. T. 2008*b*. A study on the thermal conductivity of compacted bentonites. Applied Clay Science, **41**: 181-189.

Tang, C.S., Tang, A.M., Cui, Y.J., Delage, P., Barnichon, J.D., Shi, B., 2011. A study of the hydro-mechanical behaviour of compacted crushed argillite. Engineering Geology, **118** (3-4), 93 – 103.

Van Geet, M., Volckaert, G., Bastiaens, W., Maes, N., Weetjens, E., Sillen, X., Vallejan B. and Gens, A. 2007. Efficiency of a borehole seal by means of pre-compacted bentonite blocks. Physics and Chemistry of the Earth, **32**: 123-134.

Wang, J., Sui, R., Chen, W., Guo, Y. H., Jin, Y. X., Wen, Z. J. and Liu, Y. M. 2006. Deep geological disposal of high-level radioactive wastes in China. Chinese Journal of Rock

1   Mechanics and Engineering, **25** (4): 649-658.

2   Wen, Z. J. 2006. Physical property of China's buffer material for high-level radioactive waste

3   repositories. Chinese Journal of Rock Mechanics and Engineering, **25** (4): 794-800.

4   Ye, W.M., Cui, Y.J., Qian, L.X. and Chen, B. 2009. An experimental study of the water

5   transfer through compacted GMZ bentonite. Engineering Geology 108, 169 – 176.

1 **List of Tables**

5

6 **List of Figures**

21

22

23

24 **Table 1. Mineral composition of some bentonites**

Mineral	Kunigel V1 [a]	FoCa [b]	MX80 [c]	FEBEX [d]	GMZ [e]
Montmorillonite (%)	46-49	80% (interstratified smectite/kaolinite)	79	92±3	75.4
Plagioclase (%)	—	—	9.2	2±1	—
Pyrite (%)	0.5-0.7	—	0.-	0.02±0.01	—
Calcite (%)	2.1-2.6	1.4	0.8	Traces	0.5
Dolomite (%)	2.0-2.8	—	—	0.60±0.13	—
Gypsum (%)	—	0.4	—	0.14±0.01	—
Halite (%)	—	—	—	0.13±0.02	—
Analcite (%)	3.0-3.5	—	—	—	—
Mica (%)	—	—	<1	—	—
Feldspar (%)	2.7-5.5	—	2.0	Traces	4.3
Cristobalite (%)	—	—	—	2±1	7.3
Kaolinite (%)	—	4	—	—	0.8
Quartz (%)	29-38	6	2.8	2±1	11.7
Field organic	0.31-0.34	—	0.1	0.35±0.05	—

25 *[a] JNC (2000); [b] Guillot et al. (2002); [c] Montes-H. et al.(2003); [d] ENRESA (2000); [e] Wen*

26 *(2006).*

1 **Table 2. Physical properties of some bentonites**

Parameter	Kunigel V1[a]	FoCa[b]	MX80[c]	FEBEX[d]	GMZ[e]
particle < 2μm (%)	64.5	—	60	68	60
CEC(meq/100g)	73.2	54	82.3	102[j]	77.30
Base cations exchange	Na-Ca	Ca	Na	Ca-Mg	Na-Ca
w_L (%)	474	112	519	102	313
w_P (%)	27	50	35	53	38
I_P	447	62	484	49	275
ρ_s (Mg/m^3)	2.79	2.67	2.76	2.70	2.66
S (m^2/g)	687	300	522	725	570

2 *[a] Komine (2004); [b] Marcial et al. (2002); [c] Tang and Cui (2005); [d] ENRESA (2000); [e] Wen*

3 *(2006).*

4

1 **Table 3. Stress paths of thermo-mechanical tests**

2

		T1	T2	T3	T4	T5	T6
Initial condition	p: MPa	0	0	0	0	0	0
	s: MPa	110	110	110	110	110	110
	T: °C	25	25	25	25	25	25
Path I	p: MPa	0.1	0	0	0	0	0
	s: MPa	110	39	9	110	39	9
	T: °C	25	25	25	25	25	25
Path II	p: MPa	50	0.1	0.1	0.1	0.1	0.1
	s: MPa	110	39	9	110	39	9
	T: °C	25	25	25	25	25	25
Path III	p: MPa		50	50	0.1	0.1	0.1
	s: MPa		39	9	110	39	9
	T: °C		25	25	60	60	60
Path IV	p: MPa				50	30	30
	s: MPa				110	39	9
	T: °C				60	60	60

3
4
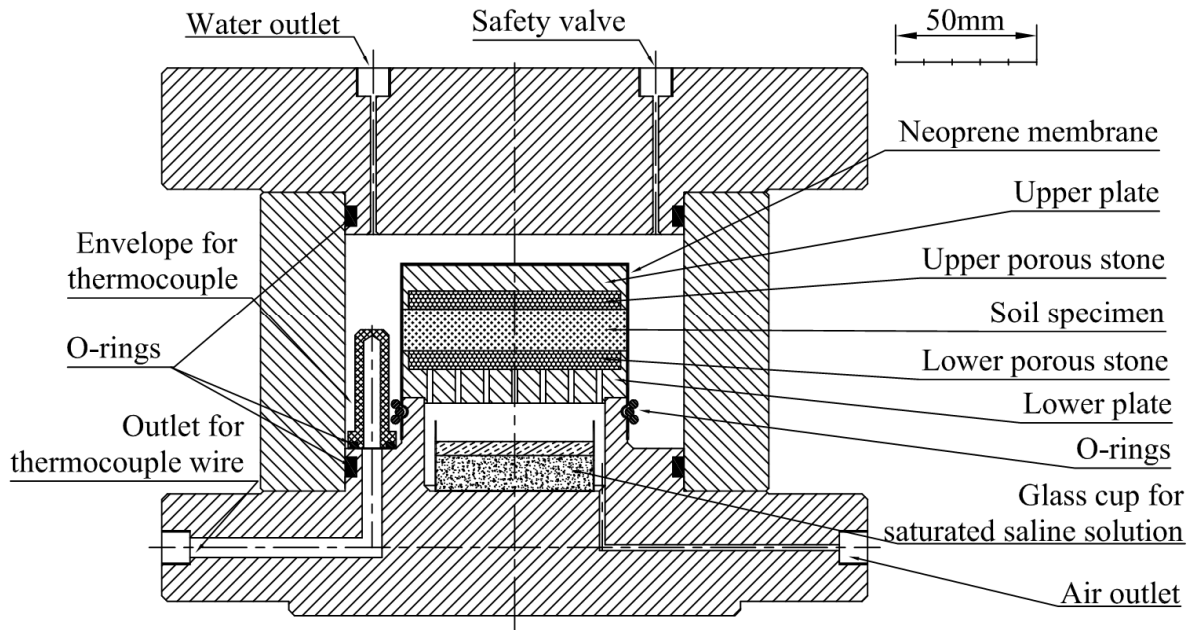
5
6 **Fig. 1. Basic scheme of the suction-temperature controlled isotropic cell (after Tang et al., 2007)**

7
8

1

2 **Fig. 2. Stress paths of tests T1-T6**
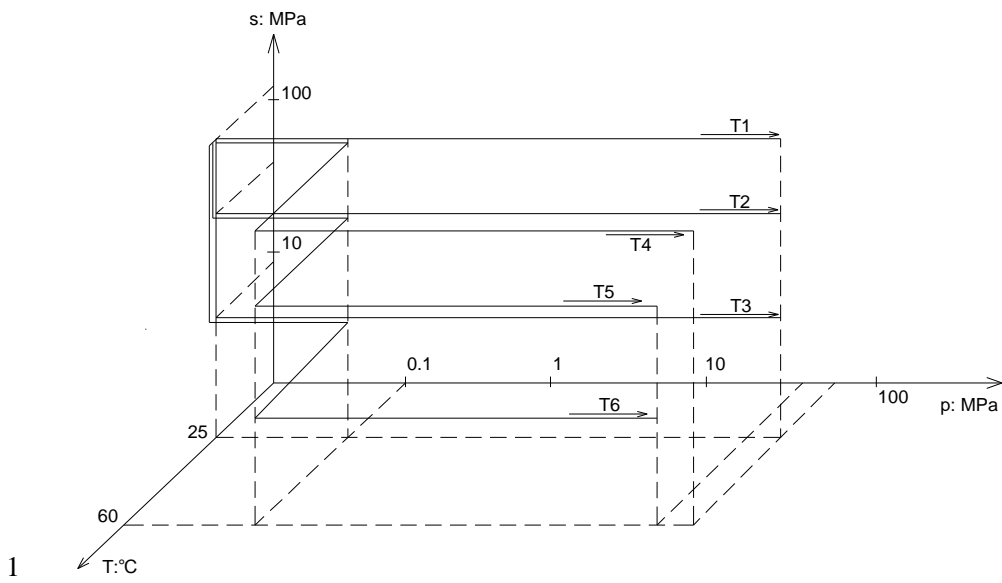
1
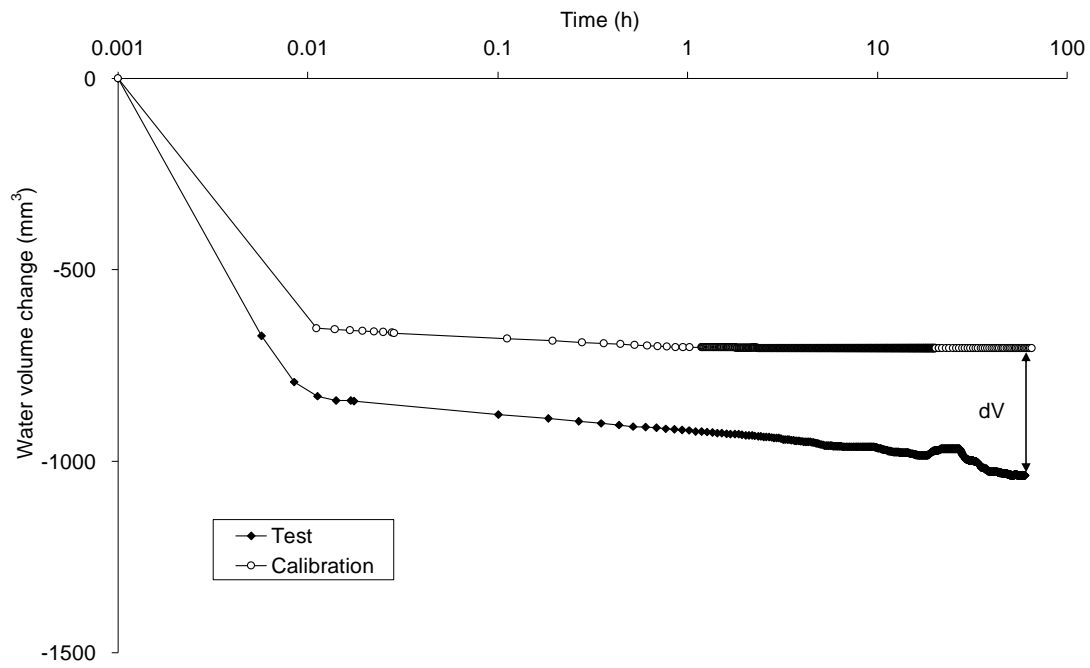
2

3   **Fig. 3. Determination of soil volume change during loading step from 1 to 2 MPa**

1

(a)

4

5   (b)
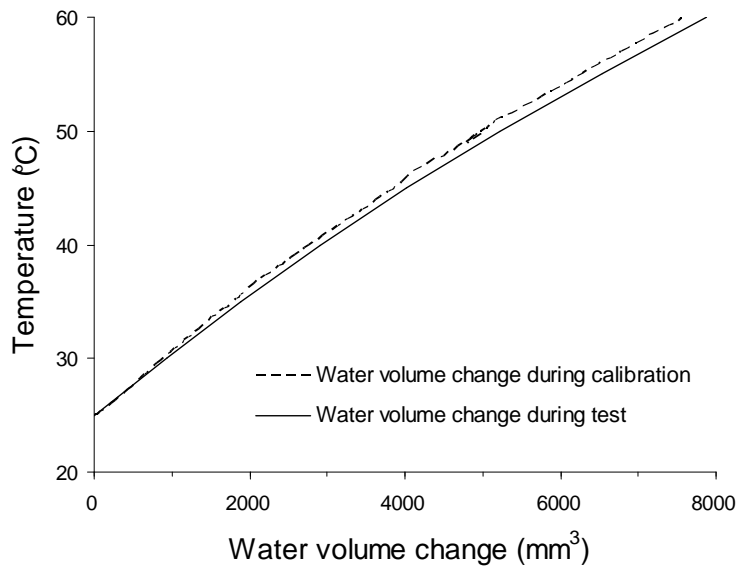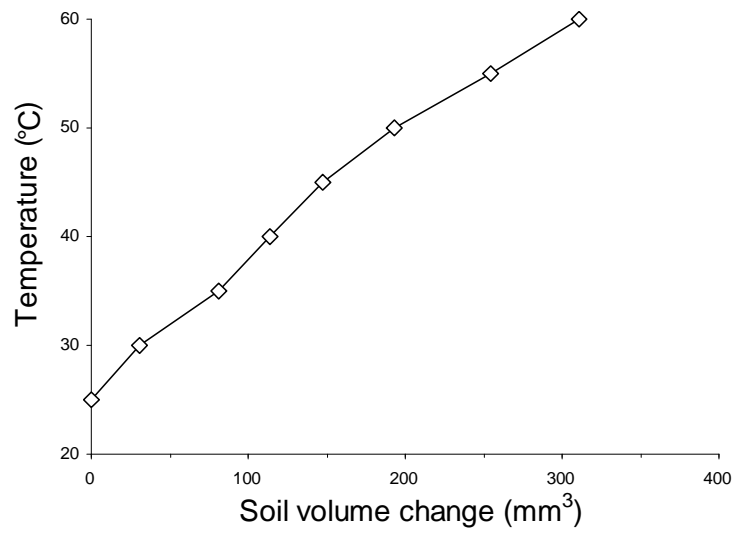
6   **Fig. 4. Determination of soil volume change during heating under confining pressure of 0.1 MPa**

Behaviour of GMZ bentonite
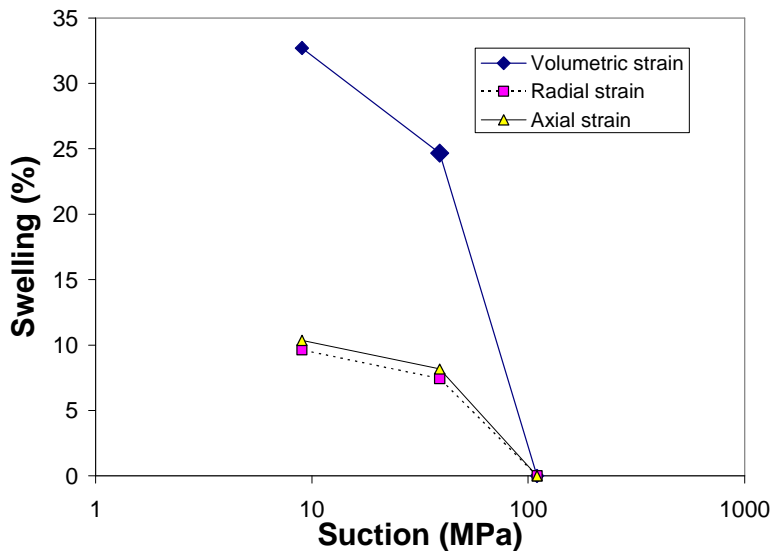
1
2   **Fig. 5. Axial, radial and volumetric strain during wetting**
3
4
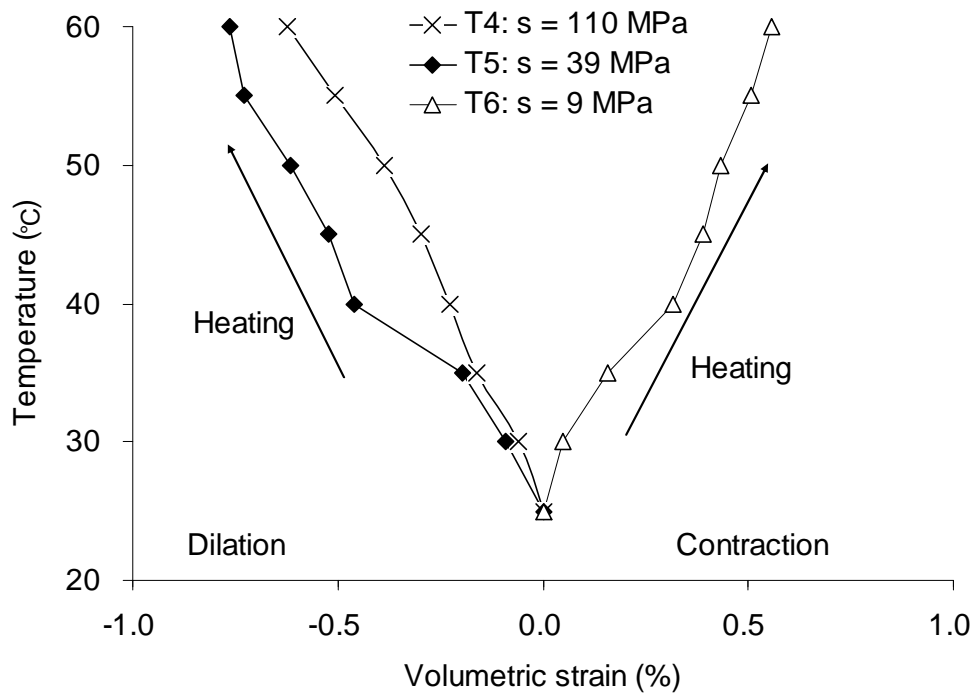
5
6   **Fig. 6. Volumetric strain during thermal loading under constant pressure at 0.1 MPa: tests T4-T6**

1

2
3 (a) s = 110 MPa

4
5 (b) s = 39 MPa

1
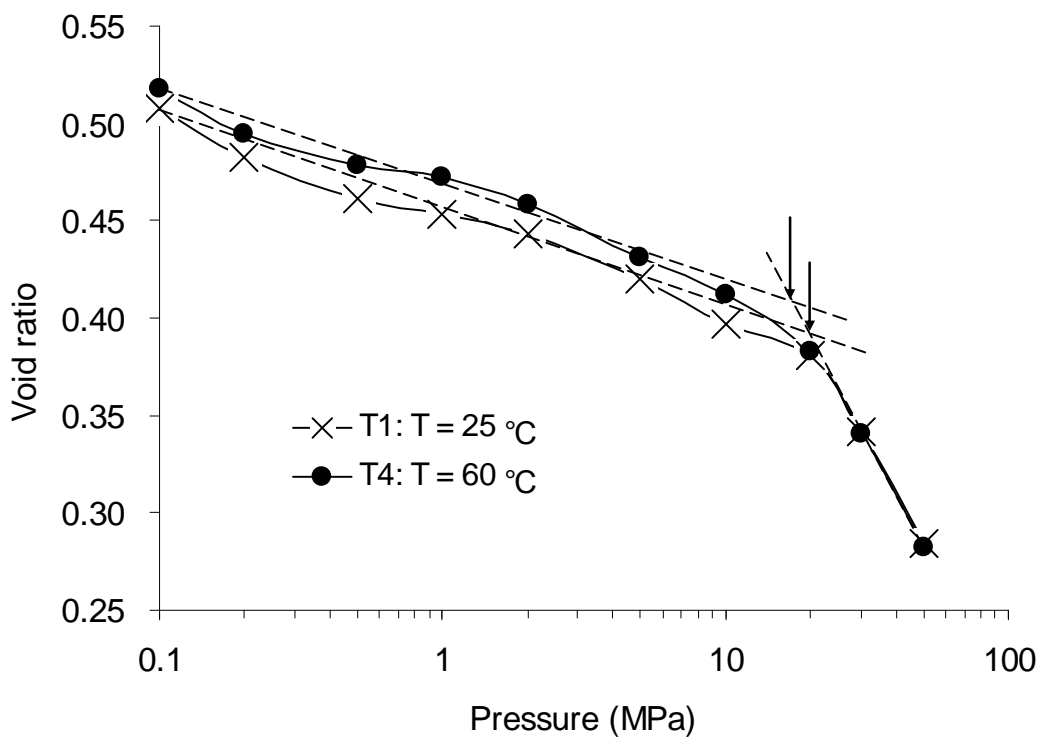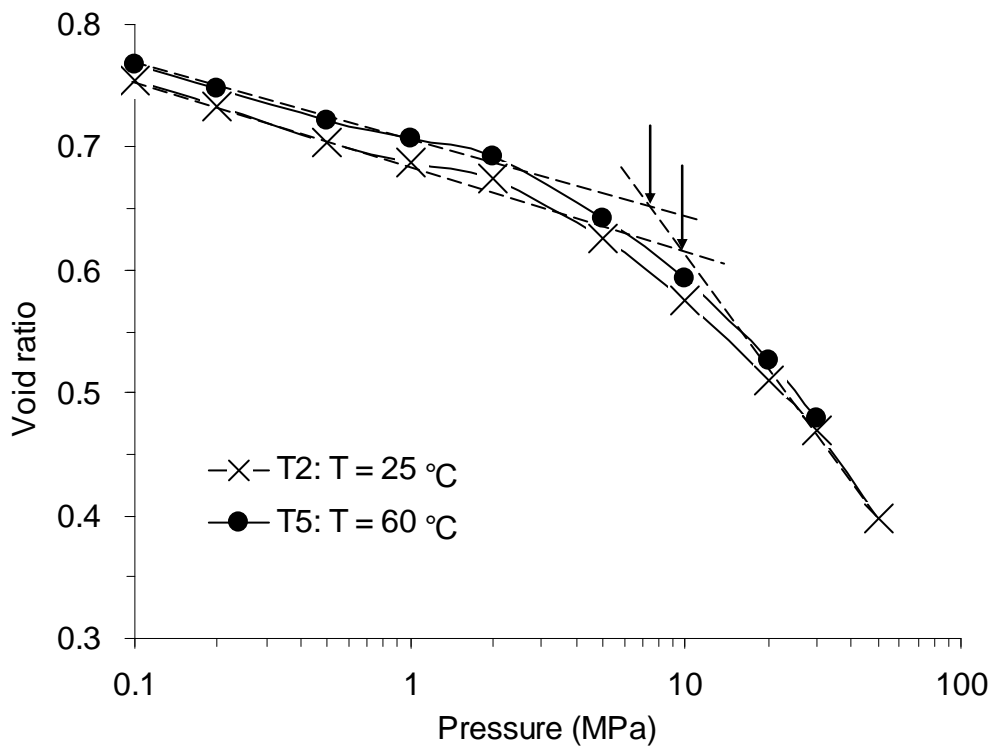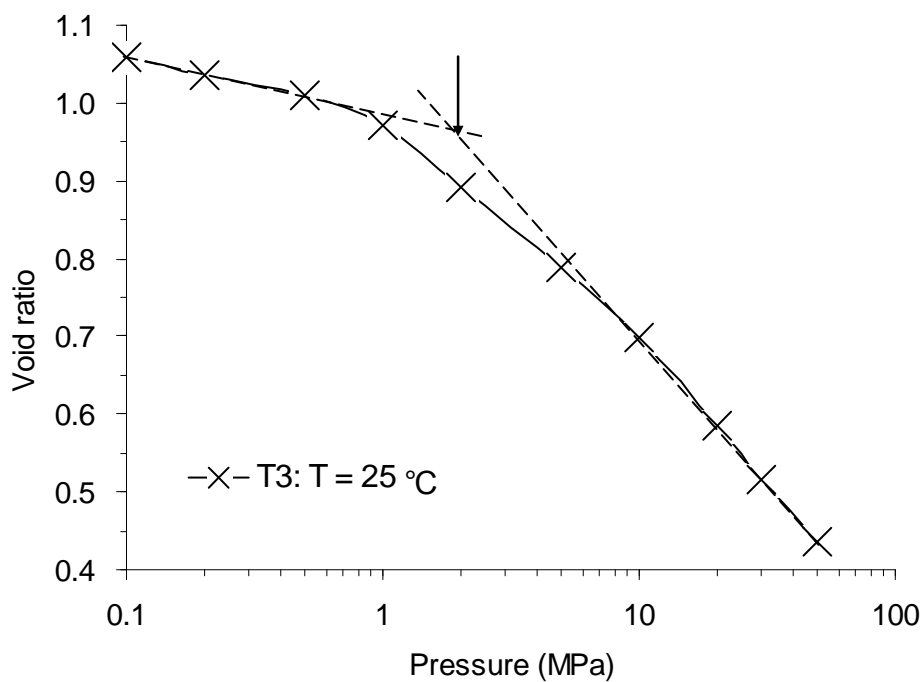
2   (c) s = 9 MPa

3   **Fig. 7. Results of mechanical loading at constant suction and temperature: tests T1-T6**

4
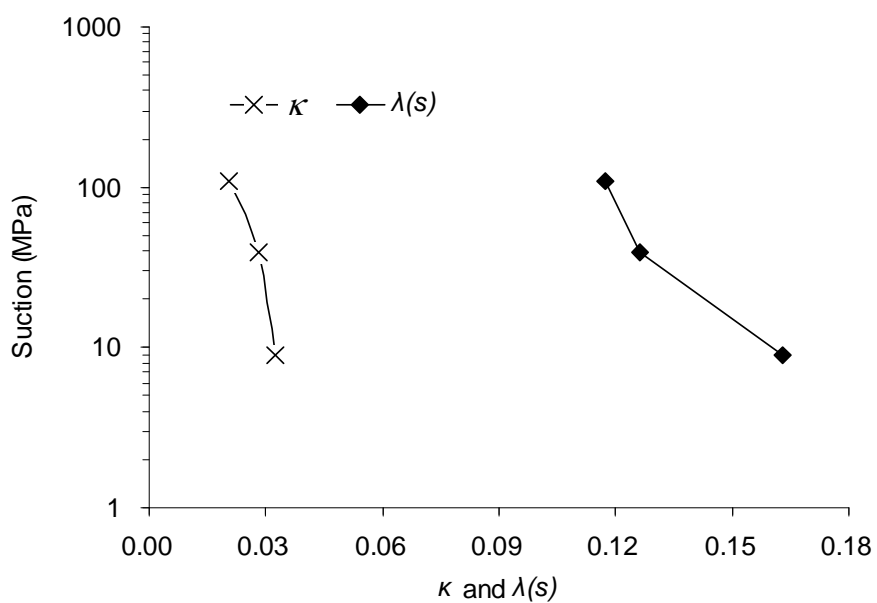
5

6   **Fig. 8. Compressibility parameters κ and λ(s) versus suction for tests at 25°C**

Behaviour of GMZ bentonite

1
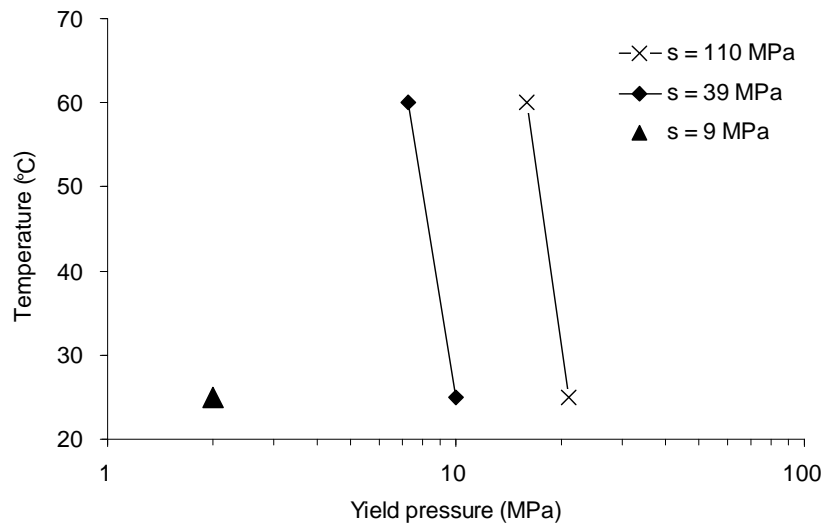
2

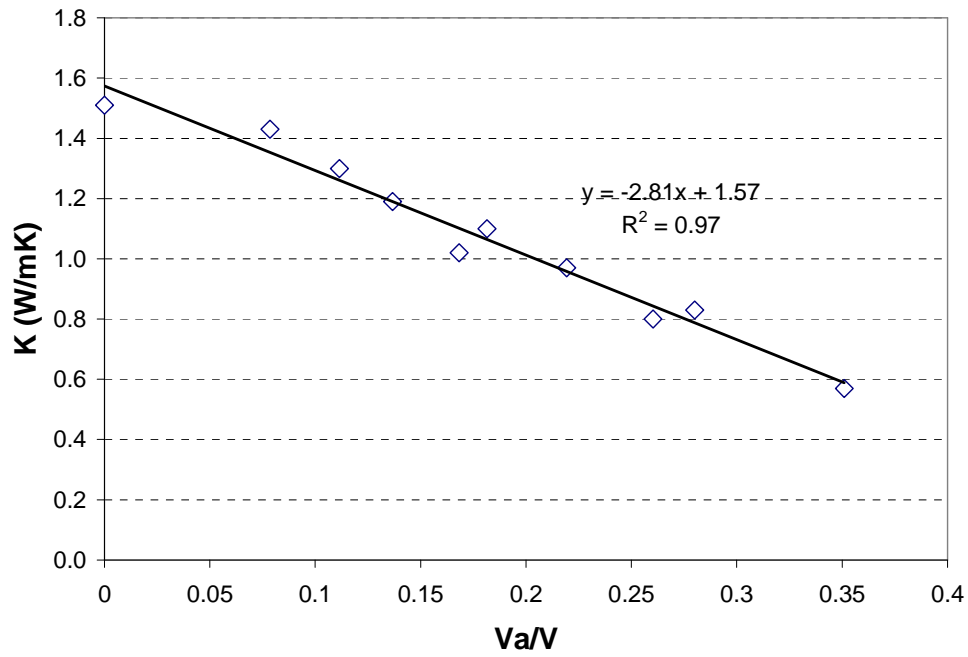3 **Fig. 9. Yield pressure p_0 versus temperature**

4
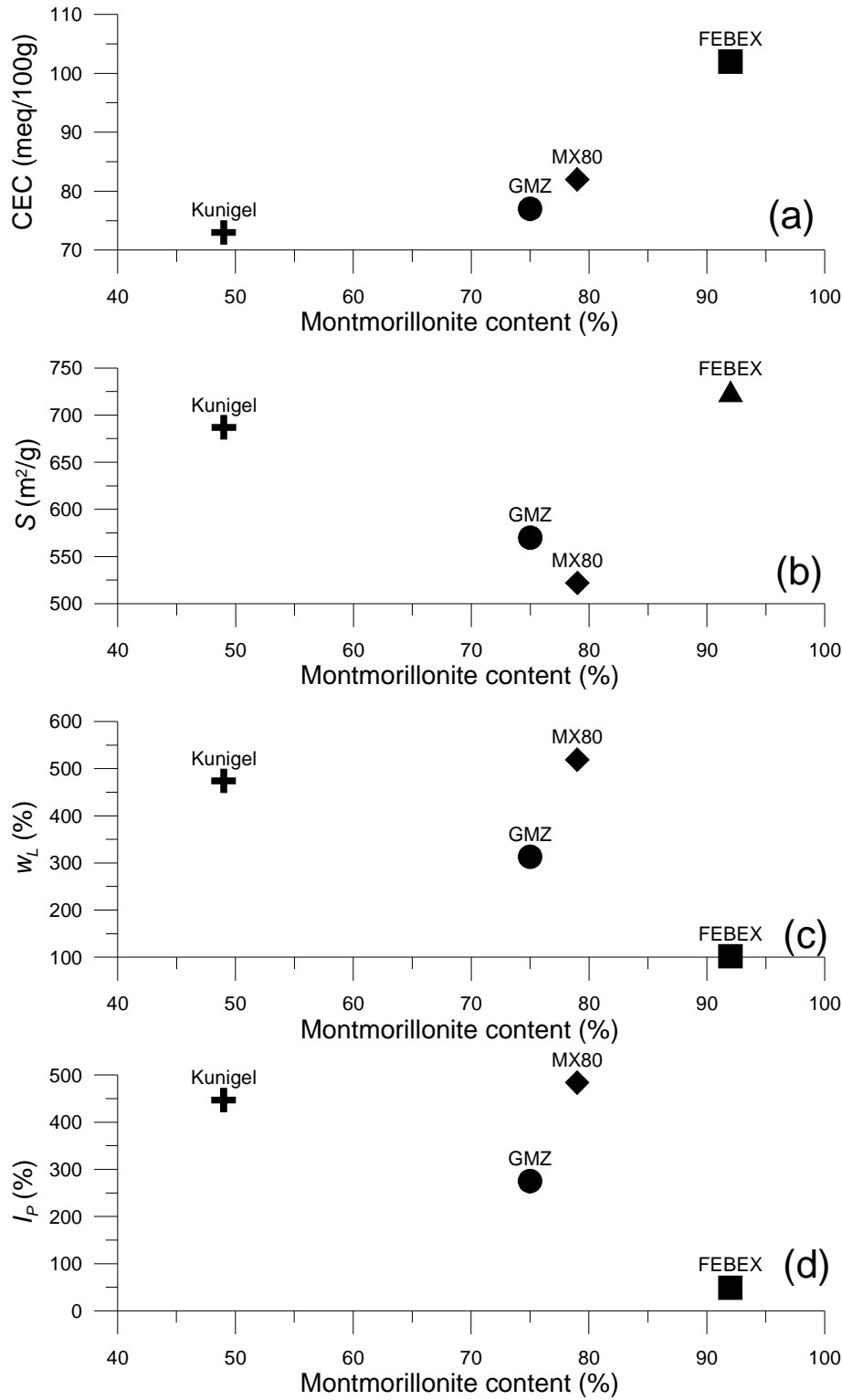
Fig. 10. Correlation between the montmorillonite content with (a) Cations Exchange Capacity, CEC; (b) specifice surface area, S; (c) Liquid limit, w_L; and (d) Plasticity index, I_P
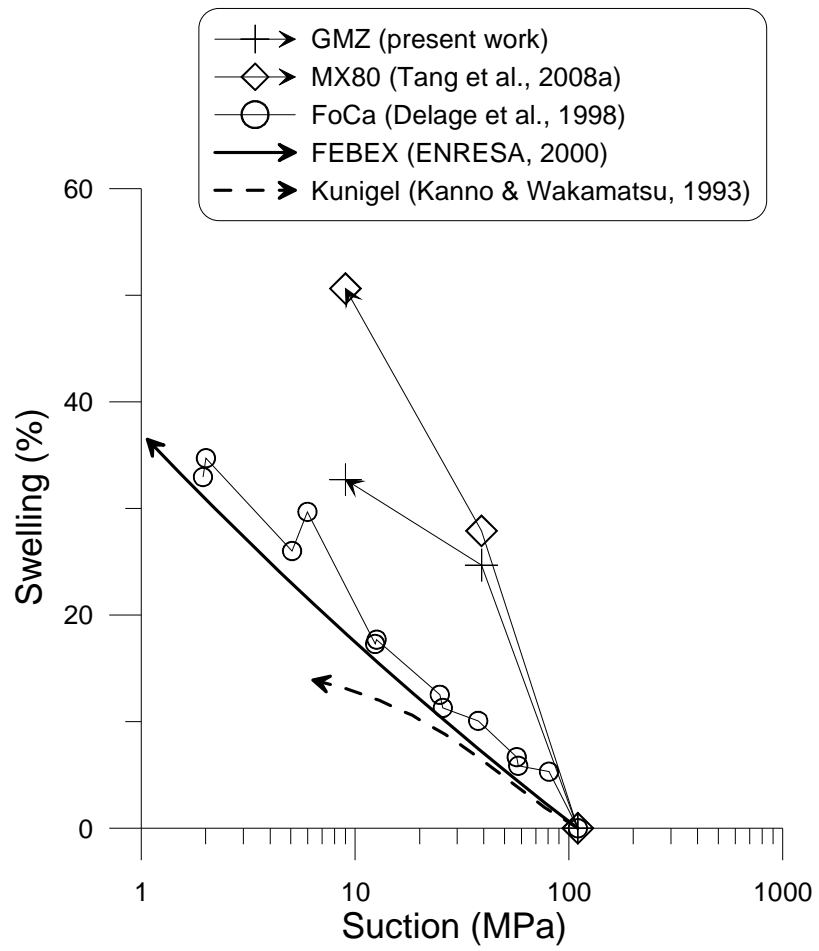
1
2
3
4
5 **Fig. 11. Variations of thermal conductivity with air-volume fraction for GMZ bentonite (after Wen, 2006)**
6

1

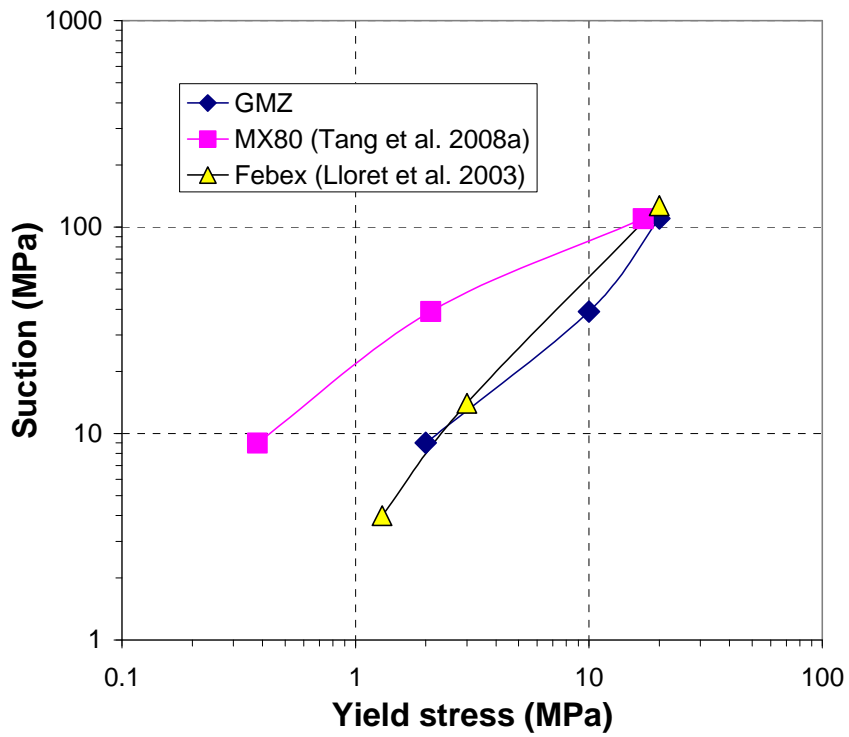**Fig. 12. Swelling of various compacted bentonite from a initial suction of 110 MPa**

3

1

2

3 **Fig. 13. Relationship between yield stress and the applied suction for various bentonites**

4

5